Monte Carlo Simulations of Salt Solutions: Exploring the Validity of Primitive Models

Zareen Abbas,* Elisabet Ahlberg, and Sture Nordholm

Department of Chemistry, Göteborg University, SE-412 96 Göteborg, Sweden

Received: September 23, 2008; Revised Manuscript Received: February 20, 2009

An extensive series of Monte Carlo (MC) simulations were performed in order to explore the validity of simple primitive models of electrolyte solutions and in particular the effect of ion size asymmetry on the bulk thermodynamic properties of real salt solutions. Ionic activity and osmotic coefficients were calculated for 1:1, 2:1, and 3:1 electrolytes by using the unrestricted primitive model (UPM); i.e., ions are considered as charged hard spheres of different sizes dissolved in a dielectric continuum. Mean ionic activity and osmotic coefficients calculated by the MC simulations were fitted simultaneously to the experimental data by adjusting only the cation radius while keeping the anion radius fixed at its crystallographic value. Ionic radii were further optimized by systematically varying the cation and anion radii at a fixed sum of ionic radii. The success of this approach is found to be highly salt specific. For example, experimental data (mean ionic activity and osmotic coefficients) of salts which are usually considered as dissociated such as HCl, HBr, LiCl, LiBr, $LiClO_4$, and KOH were successfully fitted up to 1.9, 2.5, 1.9, 3, 2.5, and 4.5 M concentrations, respectively. In the case of partially dissociated salts such as NaCl, the successful fits were only obtained in a more restricted concentration range. Consistent sets of the best fitted cation radii were obtained for acids, alkali, and alkaline earth halides. A list of recommended ionic radii is also provided. The reliability of the optimized ionic radii was further tested in simulations of the osmotic coefficients of LiCl−NaCl−KCl salt mixtures. A very good agreement between the simulated and experimental data was obtained up to ionic strength of 4.5 M.

1. Introduction

In the field of electrolyte solutions, computer simulation techniques such as molecular dynamics (MD) and Monte Carlo (MC) are emerging as important tools by which the results of theories that are more approximative in nature can be validated or refined and information not easily accessible by experiments, e.g., solvent exchange processes around an ion, can be obtained.[1−4] Although MD and MC simulations for solution models with explicit solvent provide valuable information regarding the structural and dynamical properties, computation of bulk thermodynamic properties at molecular level is problematic. In order to simulate a bulk phase, very large system size is needed and consequently such simulations consume enormous amounts of computer time. The computational efforts can be reduced significantly by taking into account the molecular ion solvent interactions only implicitly.[5−9] In such approaches, effective ion−ion and ion−solvent potentials are extracted from MD simulations[5−7] or from ionic crystal data.[8] Subsequently, activity or osmotic coefficients are calculated by using these effective potentials in MC simulations. Results of the above-mentioned studies show that agreement between the calculated and experimental mean ionic activity and osmotic coefficients is generally limited to low concentration, i.e., <1 M, except in those cases where a concentration-dependent dielectric constant[5−7] or dielectric saturation near an ion were considered.[7,8]

At a simpler level, bulk thermodynamic properties of electrolyte solutions are calculated by computer simulations considering ions as charged hard spheres of equal size dissolved in a solvent just represented by its bulk dielectric constant. This representation of an electrolyte is usually referred to in the literature as the restricted primitive model (RPM).[10] If cations and anions are considered as charged hard spheres of unequal size dissolved in a dielectric continuum, this representation is called the unrestricted primitive model (UPM).[11] Computer simulations with the RPM representation of electrolytes have been used extensively in order to predict the thermodynamic properties of electrolytes.[12−21] However, the applicability of the simulations using the RPM for predicting the ionic activity or osmotic coefficients of real salt solutions is generally restricted to concentrations ≤1 M. The UPM offers an advantage over the RPM model; i.e., ion size asymmetry is included and thus it is a step closer to the real salt solutions. It is true that electrostatic interactions between like charged ions may in a binary salt solution under certain conditions hide the individual cation and anion radii behind electrostatic correlation effects. This would mean that only the sum of these radii defining the minimal separation between cation and anion would be important, making it possible to use equal ion radii without error. However, the correlations may not be strong enough to justify this. Moreover, individual ion diameters are important in the modeling of a wide range of binary salt solutions and essentials in the treatment of mixed salt solutions.

The UPM model has been used in theories as well as in simulations in order to calculate the properties of model electrolytes.[21−36] It was found that the inclusion of ion size asymmetry has a profound effect on the predicted bulk thermodynamic properties. For example, an enhanced tendency toward ion pair formation has been seen as the cation to anion radial ratio was decreased. Rasaiah[25] found that when the RPM is used to fit the experimental data for alkali halides at low concentrations, i.e., <0.05 M, using the hypernetted chain approximation (HNC) the calculated osmotic and activity coefficients are too large at high concentrations. Changing the radius ratio while keeping the sum constant did not lead to better agreement at higher concentration. However, it was shown that

10.1021/jp808427f CCC: $40.75
Published on Web 04/02/2009

mean ionic activity or osmotic coefficients calculated by the mean spherical approximation (MSA) with the UPM can be fitted to higher concentrations as compared with the fits obtained with the RPM approximation.[37−42] From the above review it is clear that the UPM representation of electrolytes has not been fully tested in computer simulations in order to predict both ionic activity and osmotic coefficients of real salt solutions.[30]

In order to explore the validity of the primitive models with ionic radii restricted to be the same (RPM) or unrestricted (UPM), we have performed an extensive series of Monte Carlo simulations and compared our results with experiment for a wide variety of salt solutions. Such simulations are essential to find the range of applicability of RPM and UPM models of electrolytes and to provide benchmark model results for the development of simpler theory. Particularly, we have explored the possibility of mapping the mean ionic activity and osmotic coefficients calculated by the MC simulations with the UPM representation of the electrolyte onto the experimental data. The MC simulation technique offers advantages over the MSA and other theories, which have been used for such investigations, given that the ion−ion correlations due to electrostatic interactions and ion size asymmetry are included without any approximations. Thus, mapping the MC simulation results with the UPM approximation for the electrolyte onto the experimental data will serve two purposes: (i) to provide an evaluation of the applicability range in which the UPM can be used to predict the experimental mean ionic activity and osmotic coefficients for 1:1, 2:1, and 3:1 salts and (ii) to obtain reliable effective ionic radii. Effective ionic radii in the present context means the sizes of ions by which the activity and osmotic coefficients of a specific salt solution can reliably be predicted within a specific concentration range. Thus, the ionic radii obtained in this way will include effects such as electrostriction, overlapping of ion hydration shells, and excluded volume effects which become prominent at increasing electrolyte concentrations. The effective cation or anion radii obtained in this way will be very useful in simulating a wide range of phenomena occurring in electrolyte solutions such as colloidal stability, colloidal aggregation, ion adsorption, and ion transport in biological channels as well as in predicting the thermodynamic properties of mixed electrolytes such as seawater. Previously, in such investigations an ion size is given either as hydrated size, i.e., for extremely diluted system, or as crystallographic size.[43,44] The hydrated ion size chosen in this way can be very large due to the absence of overlapping between the hydration shells, which is usually present at high electrolyte concentrations.[43] On the other hand, the crystallographic radii can be very small due to the absence of hydration effects. The effective ionic radii obtained in this study will help to avoid such uncertainties. We have also demonstrated the utility of the best fitted ionic radii obtained in this study, by successfully predicting the osmotic coefficients of LiCl−NaCl−KCl salt mixtures up to an ionic strength of 4.5 M.

The article is organized as follows. In section 2 the MC simulation method is described briefly and in section 3 a procedure for converting the experimental data from molal to molar concentration scale is given. Results and discussion are provided in section 4 and conclusions in section 5.

2. MC Simulations

The MC simulation method used in this study was developed by Svensson and Woodward and has been described in detail elsewhere.[18] Here we shall summarize the main features of this method. The MC simulations were performed by the standard Metropolis algorithm.[45] A canonical ensemble was constructed by using a cubic box with periodic boundary conditions. The simulations were performed with RPM as well as UPM representation of the electrolytes. In order to attain a required concentration of electrolyte in the cubic box, the side length was varied at fixed number of total particles. To obtain activity coefficients, a modified Widom particle insertion method was used.[18] The Widom method[46] states that a nonperturbing particle α inserted at a random position $\mathbf{r}$ will have the activity coefficient γ given by

$$\ln \gamma = -\ln\langle \exp[-\beta \Delta U_{\alpha}(\mathbf{r})] \rangle_0 \quad (1)$$

The exponential term enclosed in brackets is the ensemble average of the energy change, ΔU_{α}, of adding the particle. This method provides a direct calculation of chemical potential. However, the original Widom method becomes less accurate when dealing with ionic systems of finite sizes, since the addition of a charged particle will violate electroneutrality in the cell. This effect can be reduced considerably by using very large systems but such simulations require enormous computation times. Svensson and Woodward[18] proposed a simple charge rescaling method to reestablish electroneutrality in the computation cell. This method has shown good results for symmetric as well as for asymmetric electrolytes. The thermodynamic data were in close agreement with the corresponding data generated by grand canonical Monte Carlo (GCMC) simulations.[15] Note that in GCMC simulations the problem of violation of electroneutrality in the cell does not exist because only electroneutral systems are considered. This MC simulation method with a modified Widom scheme that we use here has recently been applied to calculate the activity coefficients of ions in seawater.[47] In this MC simulation method, osmotic coefficients are calculated by the virial route.[18]

In the MC simulations reported here, large systems, i.e., 1000 ions for 1:1, 3:1, and 900 ions for 2:1 electrolytes are used. Long simulations, i.e., chains of 95 million MC configurations, were performed to generate the thermodynamic data. In the case of salt mixtures the predicted activity and osmotic coefficients were found to be dependent on the system size used in the MC simulations. However, no such size dependence was seen for systems containing 300 or more ions of each species. The simulation results reported here for the ternary salt mixture of LiCl−NaCl−KCl were obtained with 500 ions of each cationic species, i.e., a total of 3000 ions in the salt mixture.

3. Method of Data Analysis

In experimental work the properties of solutions are usually studied at constant pressure and at specified molal concentration. These conditions correspond to the Lewis-Randall (LR) representation. Theory on the other hand normally provides properties of solutions in the McMillan-Mayer (MM) representation. In the MM representation the chemical potential of the solvent is kept constant and molar concentrations are used. In order to compare with the theoretical predictions the experimental data have to be converted to molar scale or vice versa. The conversion of experimental data from molal to molar scale was performed according to the following equation[48]

$$\gamma_{\pm} = \frac{m\rho_0}{c} y_{\pm} \quad (2)$$

where m is the molality of solution, ρ_0 density of solvent (water) at 25 °C in g/cm^3), $\gamma_\pm$ the mean ionic activity coefficient in the molar (mol/L) concentration, $y_\pm$ the mean ionic activity coefficient in the molal (mol/kg) concentration, and c the molar concentration of solution. The same method of conversion is applied to osmotic coefficients.

The experimental molal concentrations (m) were converted to the molar concentrations (c) by using the following density relationship.

$$\ln \rho_s = \ln \rho_0 + \frac{AmW}{mW + 1000} \tag{3}$$

$$c = \frac{m\rho_s}{1 + 0.001\, mW} \tag{4}$$

where ρ_s is the density of solution at 25°C (g/cm^3)), A the fitting parameter, and W the molecular weight of electrolyte.

Values of the fitting parameter A for electrolytes investigated in this study are given in our previous paper.[49] The value of the constant A used for CsOH is 0.905. The experimental data (mean ion activities (ln $y_\pm$) and osmotic coefficients (ϕ)) for 1:1 electrolytes were taken from the work of Hamer and Wu[50] whereas in the case of alkaline earth halides the recommended data by Goldberg et al.,[51] were used. The experimental data for 2:1 perchlorates and 3:1 chlorides were taken from the compilation of Robinson and Stokes.[48] Experimental osmotic coefficient data of LiCl−NaCl−KCl salt mixtures were obtained from the recent measurements of Dinane.[52] The density of the salt mixture was considered to be the linear average of the densities of the single salts in the ternary salt mixture. Measured osmotic coefficients were converted from molal to molar scale by using the density of the salt mixture according to the eq 2. This procedure has been recommended by Robinson and Stokes (see page 32 of ref 48).

It is important to note that there are rigorous equations derived by Friedman[53] for converting the experimental (Lewis−Randall) activity and osmotic coefficients to theoretical (McMillan−Mayer) form or vice versa. However, the Friedman equations require knowledge of the compressibility of electrolytes and such data is only available for a few salt solutions. Simonin[54] developed approximate relations for such conversions by using the partial molal volume of the salt solution. In Simonin's equations the compressibility of salt solution was ignored and the partial molal volume was obtained by using the density of the salt solution. He obtained good agreement between the results of his and Friedman's equations for a few salts for which experimental compressibility data is available. In our previous study[55] we have tested the Simonin's equations for converting osmotic and activity coefficients calculated at the MM level by the CDH theory as well as by MC simulation to the LR system. We found negligible additional effects in fitting the theoretical data to experimental data. Therefore in our previous study[55] MM to LR conversion was performed by only using the densities of salt solutions (detailed discussion can be found in ref 55). Haynes, et al.,[56] have also shown that the effect of including the partial molal volume in the LR to MM conversion is less than 3% for an ionic diameter up to 1 nm. Moreover, in the literature[57] it has been argued that the effect due to volume change can be ignored in fitting the theoretical results to the experimental data. Thus, for the above-mentioned reasons, in this study we have performed LR to MM conversion by only using the densities of salt solutions.

4. Results and Discussion

In order to explore the validity of primitive models in predicting the activity and osmotic coefficients of real salt solutions, the MC simulation data were fitted to experimental values by adjusting ionic radii. It is important to emphasize the fact that the activity and the osmotic coefficients are simultaneously fitted; i.e., the same ionic radii are used for both properties. In order to reduce the cost of a full two-dimensional optimization, a multistep one-dimensional optimization procedure was adopted, i.e., (i) in the case of the RPM approximation for the electrolytes best fits were obtained by adjusting a mean ionic radius, (ii) in the case of the UPM approximation for the electrolytes best fits were obtained by optimizing the cationic radii while keeping the anionic radii equal to crystallographic values, and (iii) cation and anion radii were optimized by systematically changing their sizes at a fixed sum of ionic radii. A best fit between the experimental and calculated data was achieved by visual inspection. This is a tedious procedure because for each change in the ionic radius we need to calculate the activity and osmotic coefficients in the whole concentration range. In order to test the validity of the visual inspection approach, the calculated data were also fitted to the experimental data by a linear least-squares regression procedure. A fourth degree polynomial function was fitted to the calculated data, i.e., mean ionic activity (ln $\gamma_\pm$) and osmotic coefficients (ϕ) in the maximum concentration range in which a best fit to the experimental data was obtained. The polynomial function was then regressed to the experimental data without including any weighting procedure. It was found that at the maximum concentration of good fit between the calculated and experimental data the difference between the calculated and experimental ln $\gamma_\pm$ was less than 0.04 and for ϕ the deviation was less than 0.03.

4.1. Mapping the Real Salt Solutions onto the RPM. MC simulations with RPM approximation for the electrolyte were performed for a few salt solutions. Calculated mean ionic activity and osmotic coefficients were fitted to the experimental data by adjusting a mean ionic radius. The best-fitted radii and the maximum concentrations at which good fits to the experimental data were obtained are given in Tables 1 and 2. The MC results show that the applicability range of the RPM model in predicting the thermodynamic properties of real salt solutions is limited to approximately 1 M concentration. The best-fitted ionic sizes and the maximum concentration ranges obtained by the MC simulations are in very good agreement with the corresponding results obtained previously by corrected Debye−Hückel (CDH) theory (see Table 3 and Table S1 of refs 49 and 55, respectively). Thus, we may conclude that the experimental mean ionic activity and osmotic data for a number of salts can be modeled up to 1 M concentration with the RPM approximation for the electrolyte. Apparently ion size asymmetry is not very important and the screening effects essentially of linear response nature at concentrations below 1 M for these salt solutions.

4.2. Mapping Real Salt Solutions onto the UPM. Given that real salt solutions certainly will not precisely conform to the properties of even an unrestricted primitive model, it becomes important to choose an appropriate fitting procedure for the radii of the ions. It may seem as in the work of Rasaiah[22−25] that the radii are best determined at low concentrations where complicating mechanisms due to the water solvent are still of relatively minor importance. However, we are specifically interested in stretching the validity of the simple UPM as high in concentration as possible. We therefore fit our

TABLE 1: Best-Fitted Ionic Radii and Concentration Ranges Obtained by Simultaneously Fitting the Mean Ionic Activity and Osmotic Coefficients Calculated by MC Simulations with RPM and UPM Approximations to the Experimental Data[a]

salts	MC (RPM) fitted radii (nm)	max concn[b] (mol/L)	cryst[b] anion radii (nm)	MC (UPM) fitted cation radii (nm)	max concn[b] (mol/L)	ion radii ratios cation/anion
HCl	0.207	1.30	0.181	0.220	1.92	1.22
HBr	0.216	1.40	0.196	0.225	2.50	1.15
HI	0.232	1.30	0.220	0.232	1.80	1.05
$HClO_4$	0.217	1.00	0.240	0.185	1.40	0.77
HNO_3	0.199	0.67	0.179	0.210	0.80	1.17
LiCl	0.199	1.40		0.210	1.92	1.16
LiBr	0.206	1.80		0.205	3.00	1.05
LiI	0.233	0.60		0.225	1.20	1.02
$LiClO_4$	0.226	0.96		0.200	2.50	0.83
$LiNO_3$	0.198	0.97		0.210	1.20	1.17
NaCl	0.175	0.80		0.168	0.96	0.93
NaBr	0.184	0.90		0.168	0.98	0.86
NaI	0.198	0.98		0.168	0.98	0.76
$NaClO_4$	0.180	0.40		0.102	0.49	0.43
$NaNO_3$	0.142	0.67		0.102	0.60	0.57
KCl	0.163	0.60		0.135	0.78	0.75
KBr	0.165	0.70		0.134	0.70	0.68
KI	0.185	0.40		0.134	0.40	0.61
$MgCl_2$	0.249	0.30		0.295	0.98	1.63
$MgBr_2$	0.258	0.50		0.310	1.00	1.58
MgI_2	0.270	0.40		0.309	1.00	1.40
$Mg(ClO_4)_2$	0.275	0.40		0.300	0.93	1.25
$Mg(NO_3)_2$	0.230	0.86		0.295	0.95	1.65
$CaCl_2$	0.238	0.30		0.274	0.80	1.51
$CaBr_2$	0.256	0.30		0.290	0.80	1.48
CaI_2	0.265	0.30		0.297	0.60	1.35
$Ca(ClO_4)_2$	0.258	0.57		0.265	1.10	1.10
$Ca(NO_3)_2$	0.200	0.50		0.215	0.68	1.20
$AlCl_3$	0.255	0.60		0.360	1.00	1.99
$LaCl_3$	0.240	0.50		0.320	0.97	1.77

[a] In the case of the MC simulations with RPM the same ion radius was assigned to both the cation and anion. Optimized values of cationic radii were determined by fitting the MC simulations data of UPM electrolytes to the experimental data while considering the anionic radii equal to crystallographic values. The experimental data of aqueous salt solutions were measured at 25 °C (ref 50) and MC simulations are performed at 298 K. [b] max concn = maximum concentration. cryst = crystallographic.

TABLE 2: Best-Fitted Cation and Anion Radii Obtained by Fitting the MC Simulation Data of UPM Electrolytes to the Experimental Data[a]

salts	MC (RPM) fitted radii (nm)	max concn (mol/L)	MC (UPM) anion radii (nm)	cation radii (nm)	max concn (mol/L)
NaF	0.144	0.4	0.133^{C}	0.154	0.40
NaF			0.185	0.102^{C}	0.40
NaF			0.119	0.168^{H}	0.40
KF	0.169	0.98	0.133^{C}	0.198	1.00
KF			0.193	0.138^{C}	1.00
KF			0.197	0.134^{H}	1.00
RbF	0.185	0.8	0.215	0.149^{C}	0.70
CsF	0.196	0.6	0.210	0.170^{C}	0.50
LiOH	0.112	0.5	0.133^{C}	0.090	0.80
LiOH			0.154	0.069^{C}	1.00
LiOH			0.015	0.200^{H}	1.00
NaOH	0.174	0.98	0.133^{C}	0.205	1.00
NaOH			0.230	0.102^{C}	0.60
NaOH			0.173	0.168^{H}	1.20
KOH	0.188	2.4	0.133^{C}	0.230	2.50
KOH			0.225	0.138^{C}	3.00
KOH			0.229	0.134^{H}	2.50
CsOH	0.220	0.3	0.250	0.170^{C}	0.30

[a] The results shown are for aqueous salt solutions of fluorides and hydroxides. max concn = maximum concentration. The superscript C and H in columns 4 and 5 denote crystallographic and hydrated, respectively.

ionic radii to experimental data over as wide a range as possible but always including the low concentrations. At the lowest concentrations the electrostatic interactions clearly dominate the activity and osmotic coefficients and, as noted above, the size asymmetry is not strongly expressed in the properties which can be accurately fitted by a restricted primitive model. At higher concentrations, excluded volume effects due to ion size start to become more important and the properties more sensitive to the size asymmetry. We shall determine the ionic radii from a simultaneous fit of both mean activity and osmotic coefficients. It is true that these two properties are closely related through the Gibbs−Duhem relation. This relation applies both to

experimental data and to the MC simulation data internally within each data set but when we want to assess the validity of the UPM it is still necessary to compare with both activity and osmotic coefficient data to be able to determine the concentration range of validity with reasonable confidence. The Gibbs−Duhem relation may well expand the error so that the apparent range of validity from a comparison of only one of the two properties significantly overestimates the accuracy with respect to the other property. For these reasons we have chosen to consider both activity and osmotic coefficient data over a range from 0.001 M to c_{max} where c_{max} is as large as possible given that both properties shall be well reproduced in the concentration range.

4.2.1. Optimization of Cation Radii. An important deficiency in the RPM is the neglect of ion size asymmetry. As discussed in the introduction, the inclusion of ion size asymmetry even in a simple linear integral equation theory, i.e., the MSA, leads to an extension in its applicability range for real salt solutions.[37−42] Here we report the results of MC simulations including ion size asymmetry and compare with the corresponding experimental data. Ionic activity and osmotic coefficients calculated by the MC simulations with the UPM for the electrolyte were fitted to the experimental data by adjusting the cation radius while keeping the anion radius fixed at its crystallographic value. The best-fitted cation radii and concentration ranges in which a good agreement between the MC and experimental data was achieved are given in Table 1. In order to illustrate the quality of the fit obtained, the best-fitted curves for HBr, LiBr, and NaBr are shown in Figure 1a,b, and in Figure 2a,b the fitted curves obtained for $MgCl_2$ and Mgl_2 are given.

Some general trends can be inferred from the results presented in Table 1. The MC simulations with UPM approximation for the electrolyte are successful in describing the experimental data to considerably higher concentrations as compared with the fits obtained by using the RPM (Table 1, also see Table 3 and Table S1 of refs 49 and 55, respectively). This enhancement in the applicability range is particularly seen for salts which are generally considered dissociated such as chlorides and bromides of Li, Mg, as well as HCl, and HBr. On the other hand, in the case of salt solutions which are considered to be partially associated such as $NaNO_3$ and KI there was negligible enhancement in the applicability range. The root cause of these effects can be found in the patterns of ionic hydration. Bernal and Fowler[58] and later Frank[59] classified the ions as structure makers or structure breakers depending upon their hydration. Small highly charged ions which intensify the structure of solvating water molecules were classified as structure makers and conversely larger weakly charged ions which disturb the ordered structure of water around them were classified as structure breaker ions. The cations and anions with decreasing structure maker character can be arranged as given below.

$$Al^{3+} > Mg^{2+} > Ca^{2+} > H_3O^+ > Li^+ > Na^+ > K^+ > Rb^+ > Cs^+$$

and

$$F^- \cong OH^- > Cl^- > Br^- > I^- \cong NO_3^- > SO_4^{2-}$$

Gurney[60] observed the relationship between the structure maker and structure breaker character of ions and the activity coefficients of their salt solutions. He concluded that the more similar the anion and cation are in their influence on water

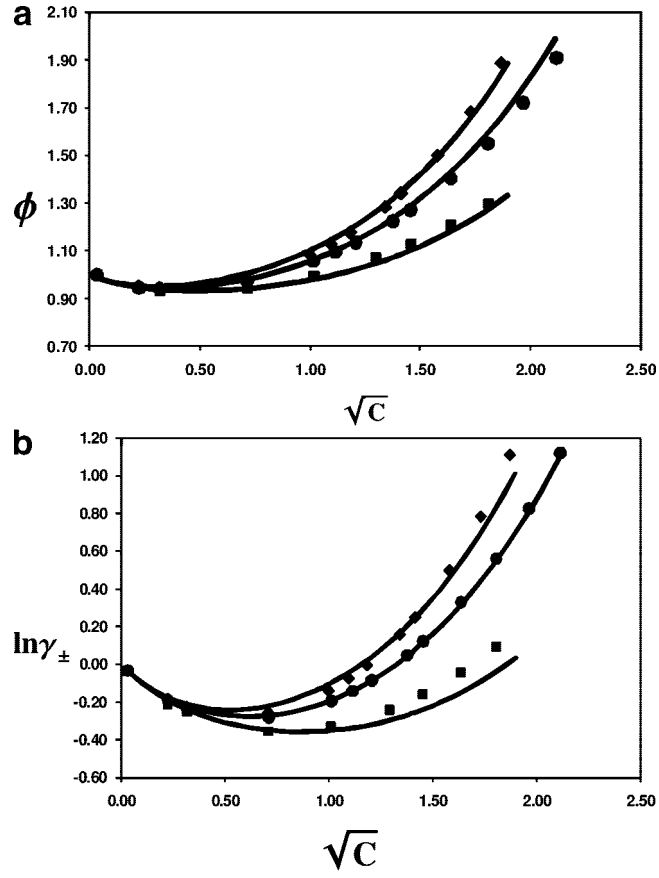

Figure 1. (a) Best-fitted curves obtained by simultaneously fitting the mean ionic activity and osmotic coefficients obtained by the experimental data with UPM approximation of electrolytes to the MC simulations data. The full lines (−) denote the experimental data whereas squares (■), circles (●), and diamonds (◆) denote the MC simulations data of NaBr, LiBr, and HBr, respectively. Osmotic coefficients (ϕ) are shown with respect to electrolyte concentration. Concentration (C) is given in moles per liter. (b) Same as in (a) but natural logarithms of mean ionic activity coefficients ($\ln \gamma_\pm$) are shown.

structure the lower lying are their mean ionic activity coefficient ($\gamma_\pm$) data. Terms such as ion association or ion pairing are usually used to describe this low-lying behavior of the mean ionic activity coefficients ($\gamma_\pm$) of salt solutions.[1] It is important to note that ion association or ion pairing are very general terms, which are used in order to describe the combined effects of ionic hydration, ion−ion electrostatic interactions and ion−solvent dispersion interactions.

Trends seen in the bulk thermodynamic properties of salt solutions may be related to the nature of the ion−water interactions at a molecular level. For example, the dielectric spectroscopic data[61] show that interactions of K^+ and Cs^+ with their hydration shells are too weak to cause irrotational binding of water molecules whereas the Na^+ ion has stronger interaction with its hydration shells. It was argued that ion pairing is present in the CsCl solution but the extent of ion pairing could not be determined. Recent neutron diffraction data with hydrogen isotope substitution in aqueous solutions of NaCl and KCl[62] also show that in the hydration shell of K^+, water molecules are orientationally more disordered than those hydrating a Na^+ ion. Experimentally measured mean ionic activity coefficients of KCl are lower than those of NaCl in a specified concentration range, i.e., 0.1−2 M.[48] This trend indicates that the differences in the bulk thermodynamic properties are due to the different hydration patterns of Na^+ and K^+ ions. However, the situation at the

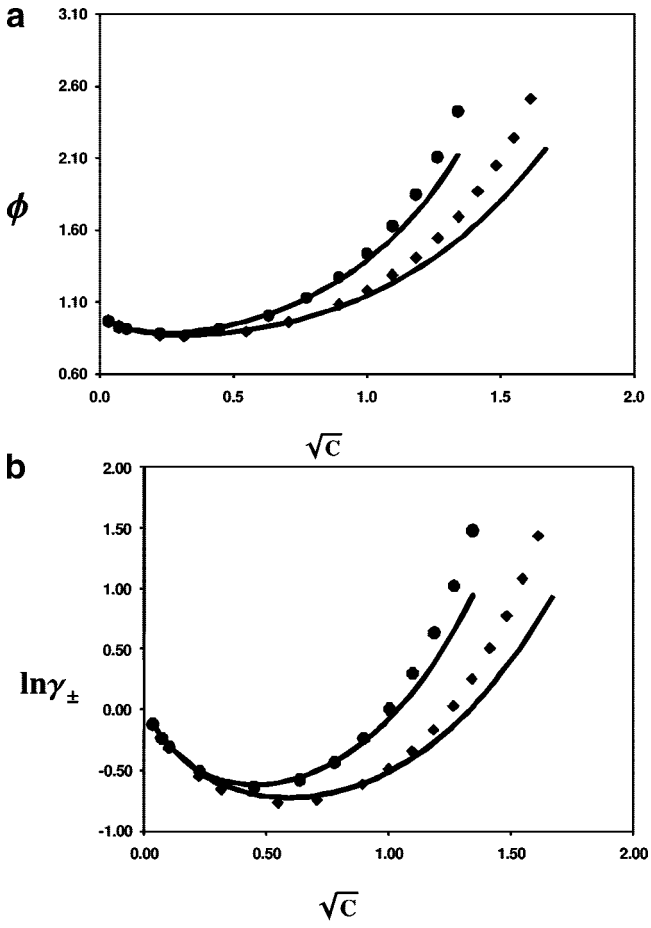

Figure 2. (a) Best-fitted curves obtained by simultaneously fitting the mean ionic activity and osmotic coefficients obtained by the MC simulations with UPM approximation of electrolytes to the experimental data. The full lines (—) denote the experimental data whereas diamonds (◆) and circles (●) denote the MC simulations data of $MgCl_2$ and MgI_2, respectively. Osmotic coefficients (ϕ) are shown with respect to electrolyte concentration. Concentration (C) is given in moles per liter. (b) Same as in (a) but natural logarithms of mean ionic activity coefficients (ln $\gamma_{\pm}$) are shown.

molecular level may be more complicated as pointed out in refs 4 and 62. For example, in experimental measurements the effect of ionic charge on the solvating water molecules was only seen in the first hydration shell and the rigidity of this hydration shell, i.e., the residence time of water molecules, was pointed out to be an important property. Our comparison of the MC simulation data with the experimental data is based only on the adjustment of ionic radii. Therefore, effects of ion association will appear in the magnitude of the optimized radii. Results presented in Table 1 clearly show such trends; i.e., in cases where the cation is a structure maker and the anion is a structure breaker such as HCl, HBr, LiCl, LiBr, etc. the MC simulations with the UPM approximation can reproduce the experimental data up to high concentrations and the optimized radii are larger than the corresponding crystallographic radii (see section 4.3 for more discussion). On the other hand, in the case of partially associated systems such as KCl, KBr, and KI the optimized cation radii are similar to the crystallographic values.[63]

The dissociated or undissociated character of salt solutions also depends upon the salt concentration. A salt solution which is dissociated at low concentrations may change to be associated at a higher concentration. For example, recent near-edge X-ray absorption spectroscopy (NEXAFS) data for NaCl solutions at various concentrations have shown that at concentrations <1 M the data can be modeled by assuming dissociated ions. However, at concentrations >1 M an assumption of solvent-separated ion pairs such as $(Na^+(H_2O)_5)Cl^-$ was necessary in order to explain quantitatively the NEXAFS data.[64] Interestingly, this is the limit of the range in which a good fit between the ionic activity and osmotic coefficients calculated by MC simulations and experimental data was obtained (Table 1). In the case of Rb, Cs chlorides, bromides, and iodides the best-fitted cation radii were equal to their crystallographic values and there was no significant increase in the applicability range as compared with the RPM case. Therefore, these results are not included in Table 1. Note that no attempt was made to further optimize the radii of Rb^+ and Cs^+ in these salt solutions in order to get better fits to higher concentration. From our previous studies[49,55] it is clear that a good fit to higher concentrations can be achieved but the values of the optimized cation radii become unphysically small, i.e., much less than the crystallographic radii. The success in describing the well-dissociated salt system is due to the fact that in the UPM approximation both the ion size and charge asymmetries are included which provide a better estimation of ion−ion correlations effects. In dissociated systems these properties seem to produce the dominant effects which determine the bulk thermodynamic properties. On the other hand, in associated systems other effects such as dispersion interactions have to be taken into account in order to get better agreement with the experimental data and reliable ionic sizes. Indeed this has been illustrated by including the dispersion interactions in calculations by the HNC theory.[65] The radius of Cs^+ obtained by fitting the experimental osmotic coefficient data was found to be larger than its crystallographic radius.

4.2.2. Determining the Effective Radii of F^- and OH^-. For "small" anions such as F^- and OH^- the assumption that the anion size in an electrolyte solution is equal to its crystallographic size is not expected to be valid. Experimental investigations and MD simulations show that these ions are strongly hydrated and their effective sizes in solvent are larger than their crystallographic sizes.[2−4] Therefore, in order to simulate the activity and osmotic coefficients of alkali and alkaline earth hydroxide and fluoride salt solutions a multistep approach was adopted, i.e., (i) the anion radius was fixed to its crystallographic value and the cation radius was optimized, (ii) the cation radius was fixed to its crystallographic value and anion radius was optimized, and (iii) the cation radius was fixed to its hydrated value which was taken from Table 1 and the anion radius was optimized. The results are summarized in Table 2. In the case of the NaF and KF salts, when the radius of F^- was taken equal to the crystallographic value (0.133 nm), we found the values of the Na^+ and K^+ radii much larger than their effective hydrated radii found in other halide salts (Table 1). When the cation radii were taken equal to crystallographic values the best-fitted anion radii obtained for NaF, KF, RbF, and CsF were 0.185, 0.193, 0.215, and 0.210 nm, respectively. These results indicate that the F^- ion acquires the hydrated radius in these salt solution which is much larger than its crystallographic radius. These are plausible results because the hydrated radii found for K^+, Rb^+, and Cs^+ in other halides are nearly equal to the crystallographic values (see section 4.2.1). In the case of hydroxides when crystallographic values of cation radii were used the best-fitted OH^- ion radii found in LiOH, NaOH, KOH, and CsOH solutions are 0.154, 0.230, 0.225, and 0.250 nm, respectively. Thus, the OH^- ion is also strongly hydrated in these solutions. The approximation of taking the Li^+ radius equal to its crystallographic value may not be valid because in most of the Li salt solutions investigated the Li^+ effective hydrated

TABLE 3: Optimized Cation and Anion Radii Obtained by Fitting the MC Simulation Data of UPM Electrolytes to the Experimental Data[a]

salts	anion radii (nm)	cation radii (nm)	max concn (mol/L)	ion radii ratios cation/anion
HCl	0.191	0.210	2.30	1.10
HBr	0.206	0.215	3.00	1.04
HI	0.212	0.240	2.00	1.13
$HClO_4$	0.250	0.175	1.00	0.70
LiCl	0.191	0.200	2.50	1.05
LiBr	0.206	0.195	3.00	0.95
LiI	0.230	0.215	1.00	0.93
$LiClO_4$	0.250	0.190	2.00	0.76
LiOH	0.144	0.079	1.00	0.55
NaCl	0.191	0.158	0.80	0.83
NaBr	0.206	0.158	0.68	0.77
NaOH	0.210	0.122	1.40	0.58
KOH	0.185	0.178	4.50	0.96
$MgCl_2$	0.191	0.285	1.00	1.49
$MgBr_2$	0.206	0.300	1.00	1.46
MgI_2	0.230	0.299	0.50	1.30
$AlCl_3$	0.191	0.350	1.00	1.83
$LaCl_3$	0.191	0.310	0.80	1.82

[a] The cation and anion radii were varied at a fixed sum of ionic radii.

radius is larger than its crystallographic value (Table 1). However, when a hydrated radius of Li^+, i.e., 0.2 nm, was used the best-fitted value found for the OH^- ion in the LiOH salt solution was 0.015 nm, which is unphysically small and, of course, much less than its crystallographic value of 0.133 nm. Note that the anion radius in NaF is also less than the crystallographic value when the hydrated radius of Na^+, i.e., 0.168 nm, was used. Thus, it seems likely that in the solutions of NaF and LiOH the cations as well as the anions might be slightly hydrated.

4.2.3. Optimizing the Ionic Radii at a Fixed Minimal Interionic Distance. In order to explore further the role of ion size asymmetry the best-fitted ionic radii were obtained by systematically varying the cation and anion radii at a fixed sum of ionic radii. In other words, when anion size was increased the cation size was decreased proportionally in order to keep the sum of ionic radii constant. The starting values in the case of hydroxides and fluoride salt solutions were set equal to the sum of the crystallographic radii of cations and the best-fitted values found for OH^- and F^- as given in Table 2. For the rest of the salts the starting values were equal to the sum of the crystallographic radius of an anion and the best-fitted radius found for a cation as reported in Table 1. Results of such optimization for a few salts are shown in Table 3. For some salts such as HCl, HBr, and LiCl there was an increase in the concentration range in which a good fit to experimental data could be achieved. However, for salts such as $HClO_4$ and $LiClO_4$ this optimization procedure led to concentration ranges, which were less than the case when only the cation radius was optimized (Table 1). This result might be due to excluded volume effects which become large in the case of salts in which there is large difference between the cation and anion radii as depicted by the ionic radial ratios of these salts. In the case of $HClO_4$ this observation is in agreement with the findings of Rasaiah;[25] i.e., inclusion of ion size asymmetry in the primitive model has decreased the agreement with experiment. We note, however, that the UPM contains the RPM as a special case. Thus, there can be no disadvantage in using UPM representation if a full multidimensional optimization can be performed.

The relative merit of UPM versus RPM representation of the electrolyte depends very much on the ionic radial ratio and the sum of ionic radii. We have investigated this matter in detail by repeating the studies presented in ref 25 through MC simulations. The results are given in the Supporting Information (Figures S1 to S6). Figure S1a shows for a fixed anion to cation radial ratio, i.e., 3.6 (same as used in ref 25), the mean ionic activity coefficients calculated by UPM approach and the corresponding values obtained by RPM at a decreasing sum of ion radii. At the lowest sum of ion radii, i.e., 1.124 Å, UPM values coincide with the corresponding data obtained by RPM in the whole concentration range. In Figure S1b it is shown that deviation between the UPM and RPM already starts at a sum of ion radii equal to 1.5 nm. However, the deviation of UPM from the RPM data also depends upon the ionic radial ratio as shown in Figures S2 and S3. For example, in Figure S3 the mean ionic activity coefficients calculated at ionic radial ratios of 1.63 and 3.6 at a fixed sum of ionic radii, i.e., 1.5 Å, are compared. In the case of ionic radial ratio of 1.63 the mean ionic activity coefficients calculated by the UPM coincides with the RPM data in the whole concentration range whereas data from ionic radial ratio of 3.6 lie above the RPM. In Figure S4 it is shown that when anion to cation radial ratio is decreased from 3.6 to 1.23 at a fixed sum of ionic radii, i.e., 2.9 Å, the UPM and RPM also coincide. Note that similar results were found for osmotic coefficients. Thus, we may conclude that the deviation between the UPM and RPM in predicting the bulk thermodynamic properties of electrolytes is strongly dependent upon the ionic radial ratio as well as the sum of ion radii.

Another interesting point was explored, i.e., the possibility of determining the RPM radius for a salt as a linear average of the UPM radii of the individual ions, $r_{RPM} = (r_{+UPM} + r_{-UPM})/2$. Here UPM radii are the optimized radii obtained by best fit to the experimental data and are given in Tables 1 and 3. In Figures S5 and S6 the results for LiBr and KOH are respectively shown. The osmotic coefficients calculated by the RPM at high concentrations are clearly below the UPM data. These are plausible results because the RPM radii obtained from the optimized ionic radii are smaller than the best RPM radii given in Table 1. However, in the case of LiCl the osmotic coefficients calculated by the RPM radii obtained from optimized UPM radii were in good agreement with the results obtained by UPM as given in Table 1. On the whole, these results show that ion size asymmetry is important in order to achieve good agreement with the experimental data.

As mentioned in section 4.2.2, in the case of LiOH both ions may be partially hydrated. This hypothesis was confirmed by the optimization procedure, i.e., when both the anion and cation radii were optimized for LiOH. The optimized radii of Li^+ and OH^- in the LiOH salt solutions were 0.079 and 0.144 nm, respectively. These radii are larger than the corresponding crystallographic values. In the case of KOH the experimental mean ionic activity and osmotic coefficient data were successfully fitted up to 4.5 M concentration (Table 3, Figure 3a,b). The optimized cation and anion radii were 0.178 and 0.185 nm, respectively. Compared to the maximum concentration range obtained (3 M) when K^+ radius was set equal to its crystallographic value (Table 3), this is a considerable increase. The mean ionic activity and osmotic coefficients of alkali hydroxide solutions show an opposite trend seen in other alkali halides, i.e., LiOH < NaOH < KOH < CsOH.[48] Specific ionic conductivities of NaOH and KOH show maxima at 2.5 and 4.5 M, respectively, while LiOH does not show such a maximum. This strikingly different behavior of LiOH as compared to NaOH

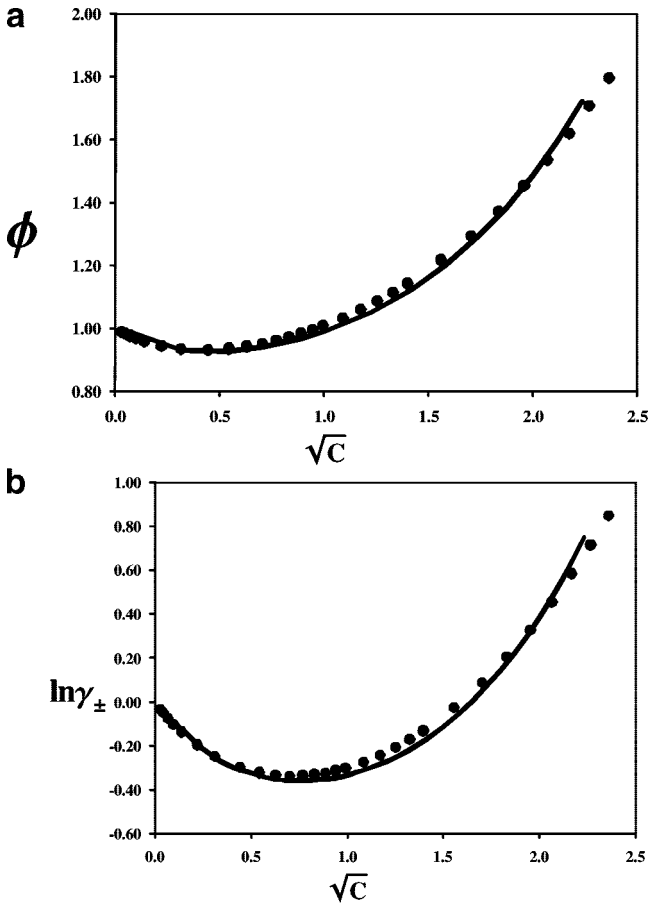

Figure 3. (a) Best-fitted curves obtained by simultaneously fitting the MC simulations data to the experimental data of KOH. Best-fitted curves were obtained by systematically varying the cation and anion radii. The full lines (—) denote the MC data whereas circles (●) denote the experimental data. Osmotic coefficients (ϕ) are shown with respect to electrolyte concentration. Concentration (C) is given in moles per liter. (b) Same as in (a) but natural logarithms of mean ionic activity coefficients (ln $\gamma_{\pm}$) are shown.

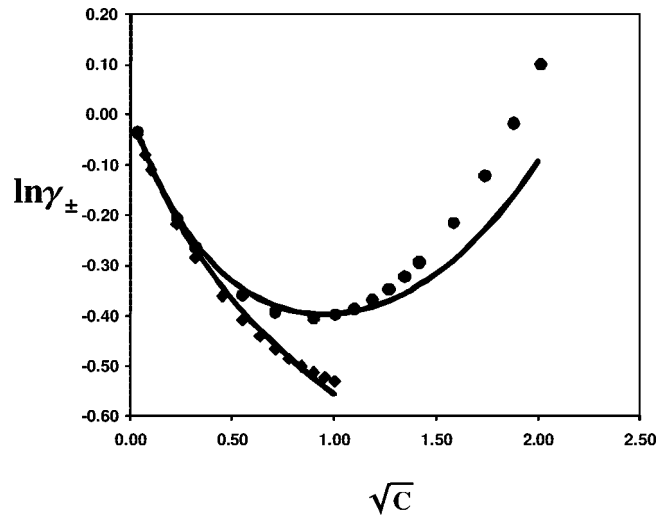

Figure 4. Best-fitted curves obtained by simultaneously fitting the mean ionic activity coefficients obtained by the MC simulations with UPM approximation of electrolytes to the experimental data. The full lines (—) denote the experimental data whereas diamonds (◆) and circles (●) denote the MC data obtained for NaF and NaOH, respectively. Concentration (C) is given in moles per liter.

and KOH has been attributed to the presence of ion pairs at all concentrations of LiOH, while in solutions of NaOH and KOH ion pairing becomes important only at concentrations higher than 2.5 and 4.5 M, respectively.[66] There is also some support for strong ion pair formation in LiOH from Raman spectroscopy.[67,68] Thus, this coincidence of maximum in conductivity of KOH at 4.5 M and a good agreement between the simulated and experimental data up to 4.5 M indicates that the KOH solution is strongly dissociated in this concentration range.

An interesting comparison can be made between the NaF and NaOH solutions. In the case of NaF when the optimized radius of Na^+, i.e., 0.168, was used the optimized F^- radius was less than its crystallographic value. However, in the case of NaOH the optimized OH^- radius was much larger than the crystallographic value when the hydrated radius of Na^+ was considered (Table 2). Comparison of experimental activity and osmotic coefficient data show that these two salt solutions are very different in nature (Figure 4). The activity coefficient versus concentration curve of NaF shows a typical behavior seen for partially associated systems; i.e., the curve decreases continuously at increasing salt concentration. On the other hand, the experimental activity coefficient data for NaOH shows the typical behavior of a dissociated system; i.e., first the curve decreases but at a certain electrolyte concentration it bends upward. Now a question arises: what are the reasons for such a difference? The experimental hydration energies and entropies of OH^- and F^- are very similar.[63] This difference can be due to the distribution of charge density in the F^-—H_2O and OH^-—H_2O clusters. The fluoride ion is a small highly charged ion and its charge density is symmetrical. In the case of OH^- the charge distribution is not symmetrical due to the presence of the O—H bond. This asymmetrical charge density distribution will then affect the ability of the ion to polarize the water molecules and hence will be manifested as a difference in their bulk thermodynamic properties.[2−4,48] Recent calculations using quantum density functional theory (DFT) show that the hydrated F^- ion is harder than the hydrated OH^- ion.[69] Hardness (n) is defined as the second derivative of the energy E of the system with respect to its number of electrons N at a constant external potential (υ) and thus is related to the electronic charge density of atoms or ions.

$$n = \frac{1}{2}\left(\frac{\partial^2 E}{\partial N^2}\right)_{\upsilon} \tag{4}$$

Recent X-ray absorption spectra of KOH reveal that the charge distribution between the OH^- and solvating water molecules is significantly asymmetric and therefore different from that for the rest of the halide anions.[70]

4.3. Physical Interpretation of the Optimized Ionic Radii. The fitted ionic radii obtained in this study represent the effective hydrated radius of an ion in a certain concentration range. The results which are shown in the Tables 1, 2, and 3 indicate that the fitted radii in the case of dissociated salts are larger than the corresponding crystallographic values but smaller than the hydrated sizes obtained from extremely diluted solutions (see Table 12 of ref 2). The cation radii obtained by fitting the simulation data to experimental data are compared for different salts in Figure 5. Consistent values are obtained for proton radii in acidic solutions as well as for Li^+, Na^+, K^+, and Mg^{2+} in their halide solutions. Triolo et al.[37] and Ebeling and Sherwinski[39] reported similar ionic radii obtained by fitting the osmotic and ionic activity coefficients calculated by the MSA to the experimental data. Good fits were obtained up to 2 M concen-

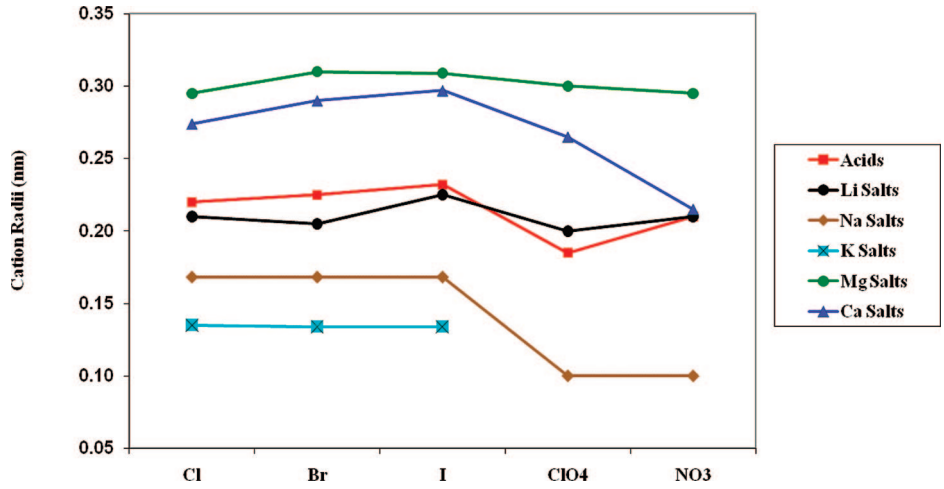

Figure 5. Comparison of the best-fitted cation radii of different salts obtained by MC simulations.

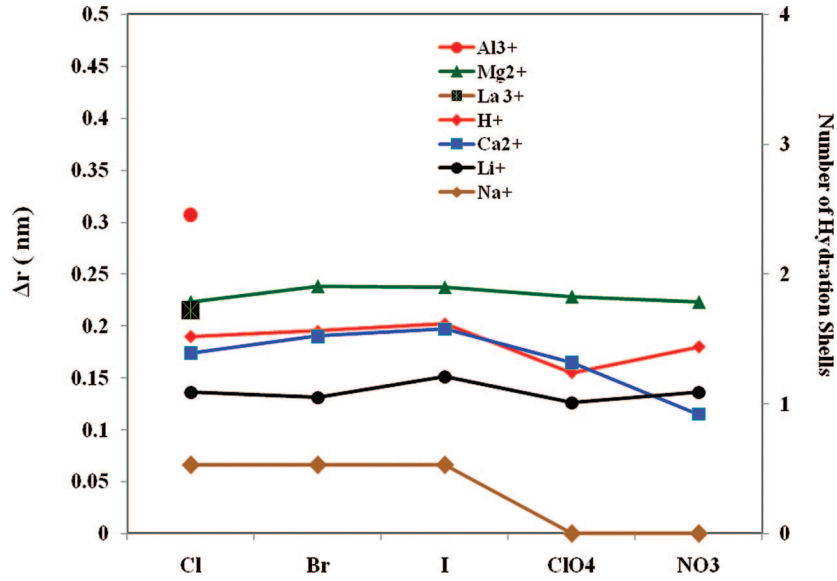

Figure 6. Difference between the crystallographic and the optimized cation radii (Δr) and the number of hydration shells of cations for different salts.

trations. However, the authors[37] mentioned that they did not fit the theoretical data between 0.1 and 0.5 M concentration. They tried to fit the data in that range but then obtained poor fits at higher concentrations.

If we consider an ion as a sphere, the difference between the crystallographic (r_c) and optimized ionic radii (r_{opt}), i.e., $\Delta r = r_{opt} - r_c$, may indicate the state of hydration of ions in different salt solutions.

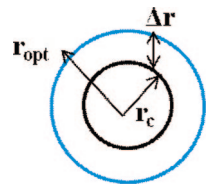

In Figure 6 the (Δr) values of cations in acids, alkali, and alkaline earth halides along with $AlCl_3$ and $LaCl_3$ are shown. The crystallographic radii of different cations are the values recommended by Marcus[63] and are given in Table 4. Note that a value for H^+, i.e., 0.030 nm, is used which is not a crystallographic value but instead calculated from thermodynamical data.[63] Ionic hydration numbers (h) based on the assumption that a hydrating water molecule has a fixed diameter are calculated by using the (r_c) and (Δr) values according to eq 5[71] and the results are given in Table 4.

$$h\left(\frac{\pi}{6}\right)d^3 = \frac{4\pi}{3}[(r_c + \Delta r)^3 - (r_c)^3] \quad (5)$$

Marcus[63] suggested a value of 0.276 nm for the diameter (d) of a water molecule near an ion and this value was used in our calculations. The hydration numbers of Mg^{2+}, Ca^{2+}, Al^{3+}, and La^{3+} obtained in this study are very similar to those reported by Marcus,[71] but we found smaller hydration numbers for the Li^+ and Na^+ ions. One reason for our lower hydration numbers is that these optimized radii represent the effective interactions of ions in concentrated solutions in which effects such as electrostriction and overlapping of hydrating layers are included. This statement is supported by the hydration numbers of Li^+, Na^+, and K^+ recently reported by Marcus.[72] He obtained considerably smaller hydration numbers for these ions when electrostriction effects were included in the model. It is interesting to note that his hydration number of Li^+ (2.3) is close

TABLE 4: Difference between the Crystallographic and Optimized Cation Radii (Δr) along with Ionic Hydration Numbers[a]

salts	cryst cation radii (nm)	MC (UPM) fitted cation radii (nm)	Δr (nm)	hydration no. h
HCl	0.030	0.220	0.190	4
HBr		0.225	0.195	4
HI		0.232	0.202	5
$HClO_4$		0.185	0.155	2
HNO_3		0.210	0.180	3
LiCl	0.069	0.210	0.141	3
LiBr		0.205	0.136	3
LiI		0.225	0.156	4
$LiClO_4$		0.200	0.131	3
$LiNO_3$		0.210	0.141	3
NaCl	0.102	0.168	0.066	1
NaBr		0.168	0.066	1
NaI		0.168	0.066	1
$NaClO_4$		0.102	0.000	0
$NaNO_3$		0.102	0.000	0
KCl	0.138	0.135	−0.003	0
KBr		0.134	−0.004	0
KI		0.134	−0.004	0
$MgCl_2$	0.072	0.295	0.223	10
$MgBr_2$		0.310	0.238	11
MgI_2		0.309	0.237	11
$Mg(ClO_4)_2$		0.300	0.228	10
$Mg(NO_3)_2$		0.295	0.223	10
$CaCl_2$	0.100	0.274	0.174	7
$CaBr_2$		0.290	0.190	9
CaI_2		0.297	0.197	10
$Ca(ClO_4)_2$		0.265	0.165	7
$Ca(NO_3)_2$		0.215	0.115	3
$AlCl_3$	0.053	0.360	0.307	18
$LaCl_3$	0.105	0.320	0.215	12
	cryst anion radii (nm)	MC (UPM) fitted anion radii (nm)	Δr (nm)	hydration no. h
NaF	0.133	0.119	−0.014	0
KF		0.193	0.060	2
RbF		0.215	0.082	3
CsF		0.21	0.077	3
LiOH	0.133	0.144	0.011	0
NaOH		0.21	0.077	3
KOH		0.185	0.052	2
CsOH		0.25	0.117	5

[a] The crystallographic size given for H^+ is obtained from thermodynamical data as explained in ref 63. cryst = crystallographic.

TABLE 5: Recommended Hydrated Ionic Radii Obtained as the Average of Best-Fitted Ionic Radii Given in Tables 1−3

ions	recommended value (nm)	valid for salts
H^+	0.214	acids except HF, H_2SO_4
Li^+	0.210	halides, $LiNO_3$, $LiClO_4$
Na^+	0.168	halides
K^+	0.134[a]	halides
Rb^+	0.149	halides
Cs+	0.170	halides
OH^-	0.198	Na and K hydroxides
F^-	0.207	K, Rb, Cs fluorides
Mg^{2+}	0.302	halides, $Mg(ClO_4)_2$, $Mg(NO_3)_2$
Ca^{2+}	0.282	halides, $Ca(ClO_4)_2$

[a] Marcus recommended a value of 0.138 nm for K^+, but our optimized value is equal to Pauling's value (ref 63).

to the value we obtained, i.e., 3. Moreover, the hydration number of K^+ was found to be 0.8, which indicates that this ion is nearly naked, a result similar to our findings (Table 4). Na^+ shows some hydration in halide salts but appears to be naked in the case of $NaClO_4$ and $NaNO_3$ (Table 1). The Na^+ hydration behavior in halides is consistent with the struture maker/breaker classification in which Na^+ is placed in between the strong structure maker Li^+ and the structure breaker Cs^+ ion.[58,59] In the case of $NaNO_3$ it is a quite established opinion that ion pairs are present and it is also apparent from the experimental mean ionic activity curve that the system is strongly correlated. Usually in such systems small ion radii are found when the data obtained by primitive models are fitted to the experimental data (Figure 6). However, in the case of $NaClO_4$ the experimental activity coefficient data do not show a typical behavior of partially associated systems.[48] There is some experimental evidence that the $NaClO_4$ solutions have stronger ion pairing than in the case of $LiClO_4$.[73] Perchlorate is a large ion; i.e., its crystallographic radius is 0.240 nm, while the Na^+ ion has a crystallographic radius equal to 0.102 nm. This large difference between the cation and anion radii may have been the major cause of good fits being restricted to low concentrations.

The hydration number of OH^- in the case of KOH found in this study is 2, which is a low value compared to a value of 4 obtained by both experiments and theory.[74] The hydration number 2 was obtained when ionic radii of both K^+ and OH^- were optimized. If we consider the ionic radius of K^+ to be equal to 0.134 nm then the optimized radius of OH^- was 0.229 nm (Table 2). According to this value the hydration number of OH^- in KOH becomes 3.8 which is nearly equal to the value of 4 reported in the literature. Thus, the hydration numbers obtained in this study should be considered as operational hydration numbers and not absolute numbers.

If we consider that the radius of a water molecule near an ion (0.138 nm) is equivalent to one hydration layer, the number of hydration shells around ions can also be extracted from the (Δr) values given in Table 4. In Figure 6 the hydration shells obtained in this way are shown. According to this criterion, Al^{3+} has two hydration shells whereas La^{3+}, Mg^{2+}, H^+, and Ca^{2+} in their halide salt solutions seem to attain a complete first hydration shell and a nearly filled second shell. The Li^+ ion shows consistently one hydration shell in all of the investigated salts. These trends are in agreement with experiment as well as results of recent ab initio MD simulations.[2−4] For example, Ikeda et al.[75] showed by first principles MD simulations that Mg^{2+} has a stable 6-fold coordination in the octahedral arrangement, in agreement with experiment. However, the hydration structure of Ca^{2+} was found to be variable.

Since we have obtained consistent sets of optimized ionic radii for a number of salts, it is possible to recommend a unique value for each ion in these different salt solutions. Recommended radii of cations as well as for OH^- and F^- are given in Table 5. These values were obtained by taking an average of the optimized ionic radii found in different salt solutions. We recommend using crystallographic radii for the Cl^-, Br^-, I^-, NO_3^-, and ClO_4^- ions (Table 1) because our results indicate that this is a good approximation in the modeling of the thermodynamic properties of electrolytes. The recommended values of ionic radii will be particularly suitable for modeling the properties of mixed electrolytes.

4.4. Simulations of Salt Mixtures. The usefulness of the optimized cation radii in predicting the thermodynamic properties of salt mixtures was evaluated for the case of a ternary salt mixture, i.e., LiCl−NaCl−KCl. Osmotic coefficients of ternary salt mixtures were calculated at different ionic strength (I) by using the optimized cation radii, i.e., 0.210, 0.168, and 0.134

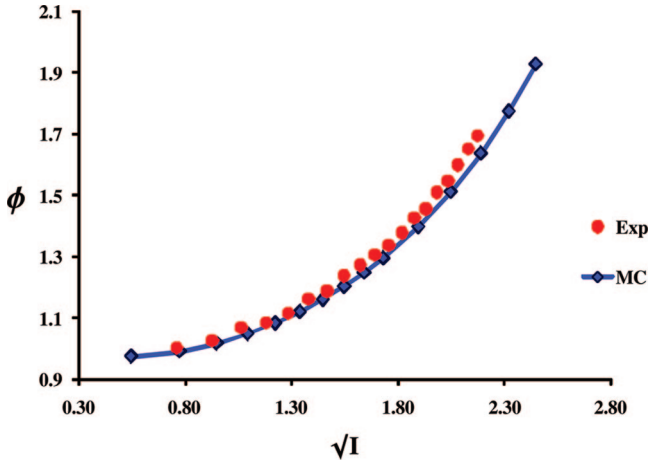

Figure 7. Experimentally determined osmotic coeffients of equimolal LiCl−NaCl−KCl salt mixtures compared with the results of MC simulations.

nm for Li^+, Na^+, and K^+, respectively, whereas the radius of Cl^- ion was set equal to 0.181 nm, i.e., the crystallographic radius. Experimental osmotic coefficient data for the LiCl−NaCl−KCl salt mixture were obtained by varying the ionic strength (I) from 0.3 to 6 molal. A mixture with a specific ionic strength (I) was obtained by mixing equimolal binary salts. For example, in a mixture of I equal to 3 each salt has a concentration of 1 molal. The simulated osmotic coefficients are compared with the measured data in Figure 7. Note that there is no fitting procedure used in this case. The good agreement between the measured and calculated data suggests that the optimized ionic radii of single salts obtained in this study will be very useful in predicting the properties of mixed salt solutions.

5. Conclusions

We have shown in this study that both ion size and asymmetry of ion sizes are significant factors in determining the thermodynamic properties of salt solutions. Our extensive MC simulations have shown that with appropriately chosen ion radii the primitive models of electrolytes can describe the experimental activity and osmotic coefficients over a wide range of concentration. Electrostatic ion−ion interactions dominate at low concentrations where the important size parameter is the minimal separation between ions of opposite charge. In this range, RPM treating the hard spheres of the same size as well as UPM works well because thermodynamic properties of salt solutions are less sensitive to the ion size asymmetry. Typically, this range is up to 1 M but less if ions are large and significantly asymmetric. The excluded volume effect causes the activity and osmotic coefficients to turn up. At this point the use of UPM can extend the fit of experimental activity and osmotic coefficients to higher concentrations often reaching well beyond 1 M. The hydration layers surrounding the bare ions are not in reality hard-sphere-like but can exhibit more complex behavior and cannot be captured in primitive models. Thus, the extension of validity achieved by use of the UPM is of very variable magnitude, sometimes very substantial while in other cases very marginal. There is, however, good reason to work with UPM representation in that we can then determine ion-specific radii. The ion-specific radii obtained in this study by mapping the calculated activity and osmotic coefficients to the experimental data seems plausible because the optimized radii fall in a physically sound range; i.e., they are larger than the crystallographic values. Moreover, consistent sets of cationic as well as anionic radii are obtained for acids, bases, and alkali and alkaline earth halide solutions, making it possible to recommend specific values of cation and anion radii. These recommended ionic radii are very useful in representing the properties of solutions of salt mixtures as indicated by the fact that a very good agreement between the experimental and calculated osmotic coefficients of LiCl−NaCl−KCl salts mixture is obtained. Thus, the ionic radii reported in this study will be very useful in predicting the thermodynamic properties of single as well as mixed salts, for example, seawater, as well as in modeling the ion transport in biological systems.

Acknowledgment. The authors are grateful to Mikael Lund and Bo Jönsson for providing the MC simulation program. Financial support has been obtained from the EU project "Nanostructures for Energy and Chemicals Production" (NENA), Contract No.NMP3-CT-2004-505906.

Supporting Information Available: Mean ionic activity coefficients calculated by MC simulations at varying sums of ion radii as well as at varying ionic radial ratios are shown in Figures S1 to S4. In Figures S5 and S6 osmotic coefficients calculated by using UPM as well as RPM are compared for LiBr and KOH, respectively. Also, the raw MC simulations data for the results given in Tables 1−3 as well as the results shown in Figure 7 are included. This material is available free of charge via the Internet at http://pubs.acs.org.

References and Notes

(1) Bockris, J. O'M.; Reddy, A. K. N. *Modern Electrochemistry*, 2nd ed.; Plenum Press: New York, 1998; Vol. 1: Ionics.
(2) Marcus, Y. *Chem. Rev.* **1988**, *88*, 1475.
(3) Ohtaki, H.; Radnai, T. *Chem. Rev.* **1993**, *93*, 1157.
(4) Bakker, H, J. *Chem. Rev.* **2008**, *108*, 1456.
(5) Lyubartsev, A. P.; Laaksonen, A. *Phys. Rev. E* **1997**, *55*, 5689.
(6) Hess, B.; Holm, C.; van der Vegt, N. *J. Chem. Phys.* **2006**, *124*, 164509.
(7) Gavryushov, S.; Linse, P. *J. Phys. Chem. B* **2006**, *110*, 10878.
(8) Lenart, P. J.; Jusufi, A.; Panagiotopoulos, A. Z. *J. Chem. Phys.* **2007**, *126*, 044509.
(9) Sanz, E.; Vega, C. *J. Chem. Phys.* **2007**, *126*, 014507.
(10) Friedman, H. L. *J. Chem. Phys.* **1960**, *32*, 1134.
(11) Carley, D. D. *J. Chem. Phys.* **1967**, *46*, 3783.
(12) Card, D. N.; Valleau, J. P. I. *J. Chem. Phys.* **1970**, *52*, 6232.
(13) Rasaiah, J. C.; Card, D. N.; Valleau, J. P. I. *J. Chem. Phys.* **1972**, *56*, 248.
(14) Valleau, J. P.; Cohen, L. K. *J. Chem. Phys.* **1980**, *72*, 5935.
(15) Valleau, J. P.; Cohen, L. K.; Card, D. N. *J. Chem. Phys.* **1980**, *72*, 5942.
(16) Van Megen, W.; Snook, I. K. *Mol. Phys.* **1980**, *39*, 1043.
(17) Rogde, S. A.; Hafskjold, B. *Mol. Phys.* **1983**, *48*, 1241.
(18) Svensson, B. O. R.; Woodward, C. E. *Mol. Phys.* **1988**, *64*, 247.
(19) Sloth, P.; Sorensen, T. S. *Chem. Phys. Lett.* **1988**, *143*, 140–144.
(20) Hanassab, S.; VanderNoot, T. J. *J. Electroanal. Chem.* **2002**, *528*, 135.
(21) Lamperski, S. *Mol. Simul.* **2007**, *33*, 1193.
(22) Rasaiah, J. C. *J. Chem. Phys.* **1972**, *56*, 3071.
(23) Rasaiah, J. C.; Friedman, H. *J. Chem. Phys.* **1968**, *48*, 2742.
(24) Rasaiah, J. C.; Friedman, H. *J. Chem. Phys.* **1969**, *50*, 3965.
(25) Rasaiah, J. C. *J. Chem. Phys.* **1970**, *52*, 704.
(26) Rogde, S. A. *Chem. Phys. Lett.* **1983**, *103*, 133.
(27) Abramo, M. C.; Caccamo, C.; Pizzimenti, G. *J. Chem. Phys.* **1983**, *78*, 357.
(28) Abramo, M. C.; Caccamo,; Malescio, G.; Pizzimenti, G.; Rogde, S. A. *J. Chem. Phys.* **1984**, *80*, 4396.
(29) Sloth, P.; Sorensen, T. S. *Chem. Phys. Lett.* **1988**, *146*, 452.
(30) Sloth, P.; Sorensen, T. S. *J. Phys. Chem.* **1990**, *94*, 2116.
(31) Svensson, B.; Åkesson, T.; Woodward, C. E. *J. Chem. Phys.* **1991**, *95*, 2717.
(32) Sorensen, T. S. *Mol. Simul.* **1993**, *11*, 1.
(33) Sorensen, T. S. *Mol. Simul.* **1993**, *11*, 267.
(34) Liano-Restrepo, M.; Chapman, W. G. *J. Chem. Phys.* **1994**, *100*, 8321.
(35) Corti, H. R.; Laria, D.; Trivani, L. N. *J. Chem. Soc., Faraday Trans.* **1996**, *92*, 91.

(36) Hanassab, S.; VanderNoot, T. J. *Mol. Simul.* **2004**, *30*, 301.
(37) Triolo, P.; Grigera, J. R.; Blum, L. *J. Phys. Chem.* **1976**, *80*, 1858.
(38) Watanasiri, S.; Brule, M. R.; Lee, L. *J. Phys. Chem.* **1982**, *86*, 292.
(39) Ebeling, W.; Scherwinski, K. *Z. Phys. Chem., Liepzig* **1983**, *264*, 1.
(40) Corti, H. R. *J. Phys. Chem.* **1987**, *91*, 686.
(41) Lu, J-F.; Xin, Y.; Li, Y. G. *Fluid Phase Equilib.* **1993**, *85*, 81.
(42) Sun, T.; Lenard, J-L.; Teja, A. S. *J. Phys. Chem.* **1994**, *98*, 6870.
(43) Conway, B. E. *Ion Hydration in Chemistry and Biophysics, Studies in physical and theoretical chemistry 12*; Elsevier Scientific Publishing Co.: Amsterdam, 1981.
(44) Collin, K. D. *Biophys Chem.* **2006**, *119*, 271.
(45) Metropolis, N.; Rosenbluth, A. W.; Rosenbluth, M. N.; Teller, A. H.; Teller, E. *J. Chem. Phys.* **1953**, *21*, 1087.
(46) Widom, B. J. *J. Chem. Phys.* **1963**, *39*, 2808.
(47) Lund, M.; Jönson, B.; Pederson, T. *Mar. Chem.* **2003**, *80*, 95.
(48) Robinson, R. A.; Stokes, R. H. *Electrolyte Solutions*, 2nd ed.; Butterworth: London, 1970.
(49) Abbas, Z.; Gunnarsson, M.; Ahlberg, E.; Nordholm, S. *J. Phys. Chem. B* **2002**, *106*, 1403.
(50) Hamer, W. J.; Wu, Y-C. *J. Phys. Chem. Ref. Data* **1972**, *1*, 1047.
(51) Goldberg, R. N.; Nuttall, R. L. *J. Phys. Chem. Ref. Data* **1978**, *7*, 263.
(52) Dinane, A. *Thermodynamics* **2007**, *39*, 96.
(53) Friedman, H. L. *J. Solution Chem.* **1972**, *1*, 386.
(54) Simonin, J. P. *J. Chem. Soc., Faraday Trans.* **1996**, *92*, 3519.
(55) Abbas, Z.; Ahlberg, E.; Nordholm, S. *Fluid Phase Equilib.* **2007**, *260*, 233.
(56) Haynes, C. A.; Newman, J. *Fluid Phase Equilib.* **1998**, *145*, 255.
(57) Myers, J. A.; Sandler, S. I.; Wood, R. H. *Ind. Eng. Chem. Res.* **2002**, *41*, 3282.
(58) Bernal, J. D.; Fowler, R. H. *J. Chem. Phys.* **1933**, *1*, 515.
(59) (a) Frank, H. S.; Evans, M. W. *J. Chem. Phys.* **1945**, *13*, 507. (b) Frank, H. S.; Wen, W. Y. *Discuss Faraday Soc.* **1957**, *24*, 133. (c) Frank, H. S. *Z. Phys. Chem. (Leipzig)* **1965**, *228*, 364.
(60) Gurney, R. W. *Ionic Precesses in Solution*; McGraw-Hill: New York, 1953.
(61) Chen, T.; Hefter, G.; Buchner, R. *J. Phys. Chem B* **2003**, *107*, 4025.
(62) Mancinelli, R.; Botti, A.; Bruni, F.; Ricci, M. A.; Soper, A. K. *J. Phys. Chem B* **2007**, *111*, 13570.
(63) Marcus, Y. *Ion Properties*; Marcel Dekker Inc: New York. 1997.
(64) Aziz, E. F.; Zimina, A.; Friewald, M.; Eisebitt, S.; Ebehardt, W. *J. Chem. Phys.* **2006**, *124*, 114502.
(65) Kunz, W.; Belloni, L.; Bernard, O.; Ninham, B. *J. Phys. Chem B* **2004**, *108*, 2398.
(66) Lown, D. A.; Thirsk, H. R. *Trans. Faraday Soc.* **1971**, *67*, 132.
(67) (a) Sharma, S. K.; Kashyap, S. C. *J. Inorg. Nucl. Chem.* **1972**, *34*, 3623. (b) Sharma, S. K. *J. Chem. Phys.* **1973**, *58*, 1626.
(68) Moskovits, M.; Michaelian, K. H. *J. Am. Chem. Soc.* **1980**, *102*, 2209.
(69) De Proft, F.; Sablon, N.; Tozer, D. J.; Geerlings, P. *Phys. Chem. Chem. Phys.* **2007**, *135*, 151.
(70) Cappa, C. D.; Smith, J. D.; Messer, B. M.; Cohen, R. C.; Saykally, R. J. *J. Phys. Chem A* **2007**, *111*, 4776.
(71) Marcus, Y. *Biophys. Chem.* **1994**, *51*, 111.
(72) Marcus, Y. *Biophys. Chem.* **2006**, *124*, 200.
(73) Frost, R. L.; James, D. W.; Appleby, R.; Mayes, R. E. *J. Phys. Chem.* **1982**, *86*, 3840.
(74) Botti, A.; Bruni, F.; Imberti, S.; Ricci, M. A.; Soper, A. K. *J. Mol. Liq.* **2005**, *117*, 81.
(75) Ikeda, T.; Boero, M.; Terakura, K. *J. Chem. Phys.* **2007**, *127*, 074503.

JP808427F